Journal of Physical and Theoretical Chemistry
of Islamic Azad University of Iran, 18 (4) 19-36: Winter 2022
(J. Phys. Theor. Chem. IAU Iran)
ISSN 1735-2126

Response Surface Methodology for Removal of Methyl Violet Dye Using *Albizia Stem Bark Lebbeck* Modified by $Fe_2(MoO_4)_3$ Nanocomposite from Industrial Wastewater

Shiva Einolghozati [1], Elham Pournamdari [2*], Nasrin Choobkar [1], Farzaneh Marahel [3]

[1] Department of Environment, Kermanshah Branch, Islamic Azad University, Kermanshah, Iran
[2] Department of Chemistry, Islamshahr Branch, Islamic Azad University, Islamshahr, Iran
[3] Department of Chemistry, Omidiyeh Branch, Islamic Azad University, Omidiyeh, Iran

Received November 2022; Accepted November 2022

ABSTRACT

The applicability of *Albizia Stem Bark Lebbeck* Modified by $Fe_2(MoO_4)_3$ nanocomposite, was studied for eliminating Methyl Violet dye from industrial wastewater. Identical techniques including (IR, XRD, and SEM) have been utilized to characterize this novel material. The impacts of variables including initial Methyl Violet concentration (X_1), pH (X_2), adsorbent dosage (X_3), and sonication time (X_4) came under scrutiny using central composite design (CCD) under response surface methodology (RSM). The values of 20 mgL^{-1}, 0.03 g, 5.0, 3.0 min were considered as the ideal values for Methyl Violet concentration, adsorbent, pH, and contact time, respectively. Adsorption equilibrium and kinetic data were fitted with the Langmuir monolayer isotherm model and *pseudo*-second-order kinetics (R^2: 0.999) with maximum adsorption capacity (120.4 mgg^{-1}), respectively. Thermodynamic parameters ($\Delta G°$: -9.26 kJ mol^{-1}, $\Delta H°$: -29.24 kJ mol^{-1}, $\Delta S°$: -131.49 kJ mol^{-1} K^{-1}), also indicated Methyl Violet adsorption is feasible, spontaneous and exothermic. Overall results confirmed that *Albizia Stem Bark Lebbeck* Modified by $Fe_2(MoO_4)_3$ nanocomposite is an effective adsorbent for removing the toxic dyes from an wastewater.

Keywords: Methyl Violet (MV) dye, Adsorption capacity, Central Composite Design (CCD), Response Surface Methodology (RSM), Industrial Wastewater

1. INTRODUCTION

The severity of water pollution has resulted from the economic development adopted by humans overall in the worldwide. Industries consume vast quantities of water and generate an enormous amount of impurities, including dyes, detergents, additives, suspended solids, aldehydes, heavy metals, non-biodegradable matter, and insoluble substances [1]. Wastewaters of industries like textile, paper, rubber, plastic, leather, cosmetic, food, and drug contain dyes, and pigments that are hazardous, and can cause skin irritation, and cancer due to the

*Corresponding author: elhampurnamdari@gmail.com

colorization of the water [2,3]. During the past few years, there has been an increasing concern regarding the residual dye in textiles, as it will be released into the environment, and resist aerobic and anaerobic conditions, heat, light, and oxidation. Residual dye is produced when an incomplete or excess of dyes onto textile fiber is incoming out during an aqueous dyeing and washing process [4]. Therefore, it is necessary to remove toxic dyes is required to safeguard human and eco-system health from industrial wastewater [5].

Methyl Violet (MV), is a basic dye, with high brilliance and intensity and is highly used in the industry. The seen show structured (MV) dye in (Fig. 1) [6,7]. Also, ingestion, inhalation, skin contact, and long-term exposure can cause eye and skin damage [8]. The harmful properties of (MV) dye create urgency from industrial wastewater before being discharged into the environment [9]. Various treatment methods must remove dyes from contaminated wastewater, including advanced oxidation processes, catalytic degradation, and adsorption. An adsorption is a promising approach owing to its simple operational design, non-susceptibility to pollutants, reusability, high efficiency, low cost, and relatively low waste production [10,11].

The adsorption method is especially suitable for solving dyes, environmental, gases, and metals problem, and has many advantages, so it has become the focus and hot spot of research. In comparison with other conventional techniques (ion exchange, biological treatments, and electrolysis), adsorption is one of the most successful and uncomplicated techniques for deletion of toxic and noxious contaminations. Its popularity is due to advantages including higher efficiency lower waste, facile, and mild operational conditions. The successfulness of adsorption techniques in deletion of pollutants especially those which are extremely stable in biological degradation process via economically accomplishable mild ways [12-18]. Thus, the extensive utilization of adsorption techniques for deletion of numerous chemicals from aqueous solutions seems logical [17,18]. In recent years, it has been tried to eliminate specified organics from water samples by applying various potential adsorbents. In this regard, magnetic nanoparticles (MNPs) have been studied extensively as novel adsorbents with large surface area, high adsorption capacity and small diffusion resistance. For instance, they have been used for the separation of chemical species such as environmental pollutants, metals, dyes, and gases [19,20]. Iron oxide nanoparticles are widely used for metal remediation due to their low toxicity and easy separation from water media in addition, where the nanoparticle (NP) is composed of magnetite, a facile magnetic separation of NPs, along with associated contaminants, can be performed. However, bare magnetite nanoparticles rapidly aggregate in aqueous systems and are highly susceptible to transformations under many environmental conditions [21-25].

The experimental conditions of pH of the solution, contact time, initial (MV) dye concentration, adsorbent dosage, and the dye removal percentage, were investigated and optimized by central composite design (CCD) under response surface methodology (RSM). The adsorption of (MV) dye follows the *pseudo*-second-order rate equation, and Langmuir's model for the equilibrium data explanation. The capability of *Albizia Stem Bark Lebbeck* Modified by $Fe_2(MoO_4)_3$ nanocomposite in eliminating (MV) dye from aqueous solutions was demonstrated by evidence.

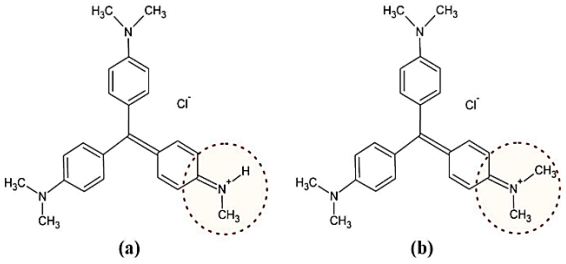

Fig. 1. The structures of Methyl Violet (MV) dye. **(a)** 2B and **(b)** 10B.

2. EXPERIMENTAL

2.1. Materials and Instrumentation

All the chemicals used are of the highest purity and purchased from Merck (Darmstadt, Germany). Methyl Violet dye (98%), the initial concentrations of this dye in the experiment were defined in relation to the amount of dye of the same type remaining in the industrial wastewater. Ammonium heptamolybdate (99%), and Iron nitrate (III) (98.0%). The applied instruments were as follow: spectrophotometer model 1601 PC (Shimadzu Company, Japan). IR (Spectra model, PerkinElmer Company, Germany). SEM (Phillips model, PW3710, Netherland), was used to study the morphology of samples. An ultrasonic bath with a heating system (Tecno-GAZ SPA Ultra Sonic System, Italy), was used for the ultrasound-assisted adsorption procedure.

2.2. Preparation of Albizia Stem Bark Lebbeck

The *Albizia Stem Bark Lebbeck* powder, this material, is a zero-value agricultural waste product. The off woody of the *Albizia Stem Bark Lebbeck* powder plant, thoroughly washed with water, and sun-dried for five days. The dried biomass was milled and then fractionated using 100-300 m analytical sieves and washed twice with 0.01 M HCl to remove any dyes on the biomass [26].

2.3. Preparation of Albizia Stem Bark Lebbeck Modified by $Fe_2(MoO_4)_3$ nanocomposite

The iron oxide-molybdenum nanocomposite was prepared in a synergistic process by mixing the juice solutions of heptamolybdate ammonium and iron nitrate mode as follows: The container with the heptamolybdate ammonium was placed, in a warm bath with a temperature of 70°C, and the iron nitrate solution was added slowly while stirring the ammonium heptamolybdate solution. Then we increased the bath temperature to 90°C. The sediment suspension was stirred for 3 hours. Stirring was stopped and the suspension was placed in the laboratory for 2 hours. The *Albizia Stem Bark Lebbeck* Modified by $Fe_2(MoO_4)_3$ nanocomposite produced suspensions were prepared from a leaf medlar with an equal weight ratio and after analysis, BET, IR, XRD and SEM were used as adsorbent [26,27].

2.4. Adsorption experiments

Generally, the sonochemical adsorption experiment was carried out in a batch mode as follows: The Erlenmeyer flask was loaded with exact quantities of (MV) dye solution (50 mL) at a specified concentration of 20 mg L^{-1} and pH of 5.0 with a known quantity of adsorbent (0.03 g), while the desired sonication time (3 min) was maintained at the 25°C. The adsorption trials were executed in mode, and the solution was ultrasonicated at conditions devised under RSM. At the end of the adsorption process, the sample solution was immediately centrifuged and the analysis of the dilute phase was done for determining (MV) dye concentration with the help of UV–Vis spectrophotometer at a wavelength of 580 nm, as shown in (Fig. 2). The equilibrium

concentrations and removal efficiency (%) of the (MV) dye were calculated according to equations (1) and (2), respectively. All experiments five times, and final results were presented as mean values.

$$R\% = \frac{C_0 - C_e}{C_0} \times 100 \quad (1)$$

$$q_i = \frac{V(C_0 - C_e)}{M} \times 100 \quad (2)$$

C_0 (mg/L) in the formula refers to the initial (MV) dye concentration, and C_e (mg/L) represents the equilibrium (MV) dye concentration in an aqueous solution. V (L) shows the solution volume, and W (g) signifies the mass adsorbent [28].

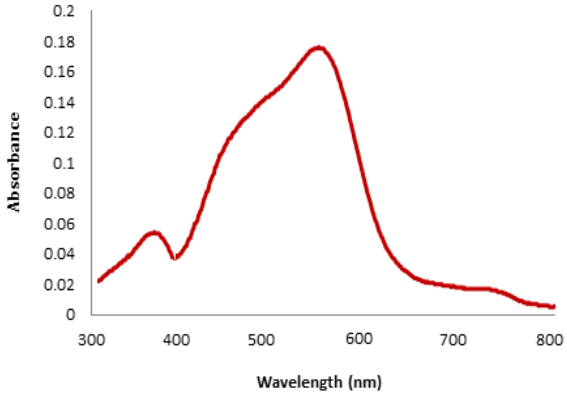

Fig. 2. Absorption spectra of (MV) dye onto *Albizia Stem Bark Lebbeck* Modified by $Fe_2(MoO_4)_3$ nanocomposite.

2.5. Central composite design (CCD)

The central composite design, for modeling, and the optimization of the effects of concentration of (MV) dye (X_1), pH (X_2), amount of adsorbent (X_3), and contact time (X_4) on the ultrasonic-assisted adsorption of MV dye by *Albizia Stem Bark Lebbeck* modified by $Fe_2(MoO_4)_3$ nanocomposite. Four levels at which the R% of (MV) dye as a response was determined and shown in (Tables 1, and 2). To evaluate the essential, and effective terms for modeling the answer based on *F*-test. *P*-values less than 0.05 are generally considered a criterion for distinguishing statistically significant variables [28,29].

Table 1. Experimental factors, levels, and matrix of CCD.

Factors	Symbol	levels			Star point α = 2.0	
		Low (-1)	Central (0)	High (+1)	-α	+α
Conc. (MV) dye (mgL^{-1})	(X_1)	10.0	15.0	20.0	5.0	25.0
pH	(X_2)	2.0	5.0	6.0	4.0	8.0
Conc. Sorbent (g)	(X_3)	0.015	0.025	0.03	0.075	0.035
time (min)	(X4)	2.0	3.0	4.0	2.0	6.0

Table 2. The design and the response.

Run	X_1	X_2	X_3	X_4	R% (MV) dye
1	10	5	0.030	3	100.0
2	10	4	0.025	4	95.0
3	15	5	0.03	3	99.1
4	10	6	0.025	4	94.0
5	20	6	0.015	5	90.4
6	10	5	0.035	2	100.0
7	10	7	0.025	6	95.0
8	15	8	0.025	4	96.0
9	15	6	0.025	4	95.0
10	15	6	0.015	4	100.0
11	20	7	0.025	6	95.0
12	10	5	0.035	2	96.0
13	15	6	0.025	4	100.0
14	15	6	0.025	4	93.0
15	10	5	0.015	6	81.8
16	15	6	0.025	4	76.8
17	20	5	0.015	6	96.5
18	15	6	0.005	4	100.0
19	20	5	0.015	2	80.0
20	10	7	0.035	2	92.5
21	20	5	0.015	2	95.0
22	20	6	0.035	2	99.2
23	15	6	0.025	4	97.5
24	10	5	0.035	4	100.0
25	15	5	0.025	6	95.0
26	10	4	0.015	6	96.0
27	5	6	0.025	4	77.7
28	10	4	0.015	6	97.7
29	10	5	0.035	4	99.1
30	15	7	0.025	2	95.0

3. RESULTS AND DISCUSSION

3.1. Characterization of adsorbent

3.1.1. BET; analysis of *Albizia Stem Bark Lebbeck* Modified by $Fe_2(MoO_4)_3$ nanocomposite

The nitrogen adsorption–desorption isotherm at 77 K onto *Albizia Stem Bark*

Lebbeck Modified by $Fe_2(MoO_4)_3$ nanocomposite is shown in (Fig. 3). The adsorption capacity with an increase in the number of adsorbed $Fe_2(MoO_4)_3$ nanocomposite, the relative partial pressure range on the adsorption isotherms gradually decreases. Because the $Fe_2(MoO_4)_3$ nanocomposite, in the composite spread into *Albizia Stem Bark Lebbeck* channels, made the channels, narrow and the pore volume decrease. By comparing the pore size distribution of the samples, it can be that with the increase in the adsorbed Fe_2 $(MoO_4)_3$ nanocomposite, the most probable pore diameter. Because, when the Fe_2 $(MoO_4)_3$ nanocomposite, was introduced into the *Albizia Stem Bark Lebbeck* channels, the most probable pore diameter reduced, indicating that the Fe_2 $(MoO_4)_3$ nanocomposite, entered the *Albizia Stem Bark Lebbeck* channels [30,31].

Table 3. Characterization Analysis BET of sorbent.

Characterization		Samples	
		Albizia Stem Bark Lebbeck	*Albizia Stem Bark Lebbeck* Modified by $Fe_2(MoO_4)_3$
	Correlation coefficient	0.9972	0.9915
BJH desorption	Surface area (m^2/g)	45.84	45.17
	Pore volume (cm^3/g)	0.9202	0.8917
BJH adsorption	Surface area (m^2/g)	90.27	89.80
	Pore volume (cm^3/g)	0.9493	0.9288

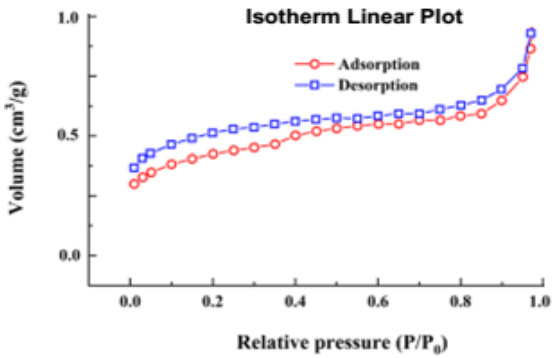

Fig. 3. N_2 gas adsorption/desorption isotherms of *Albizia Stem Bark Lebbeck* and *Albizia Stem Bark Lebbeck* Modified by $Fe_2(MoO_4)_3$ nanocomposite.

3.1.2. IR, XRD, and EDX analysis

Fig. 4a; Demonstrates the IR spectrum of *Albizia Stem Bark Lebbeck* Modified by $Fe_2(MoO_4)_3$ nanocomposite. While the broad signals at 1016.45-1059.99 cm^{-1} is ascribable to C–H stretching from phenolic and alcoholic groups, the one at 776.5 cm^{-1} is attributable to Fe–O. Also the apparent signals at 3101.21 cm^{-1} and 3418.89 cm^{-1} are attributable to C–OH stretching [26,27]. Fig. 4b, represents the X-ray diffraction of the *Albizia Stem Bark Lebbeck* Modified by $Fe_2(MoO_4)_3$ nanocomposite adsorbent. The peaks at at 2θ= 21.45°, 33.0°, 37.2°, 44.75°, 56.0° and 62.0° belong to the lattice planes of at (111), (220), (311), (400), (440), and (511), confirming the cubic structure of *Albizia Stem Bark Lebbeck* Modified by $Fe_2(MoO_4)_3$ nanocomposite. However the great intensity of signal at 37.2°(311) confirmed that there is a slight amount of amorphous state material. Indeed, the perfect synthesis of MgO-SiO_2NPs can be judged through looking at its XRD pattern [32]. The energy-dispersive X-ray spectroscopy (EDX) spectrum of *Albizia Stem Bark Lebbeck* is exhibited in (Fig. 4c). It is worthy of note that, functionalized *Albizia Stem Bark Lebbeck* Modified by $Fe_2(MoO_4)_3$ nanocomposite became uneven. In (Fig. 4d), the EDX spectrum of *Albizia Stem Bark Lebbeck* Modified by $Fe_2(MoO_4)_3$ nanocomposite is shown [32,33].

3.1.3. Surface morphology

The morphological properties of *Albizia Stem Bark Lebbeck* Modified by $Fe_2(MoO_4)_3$ nanocomposite was investigated by SEM and is exhibited in (Fig. 5). The evenness, homogeneity, orderliness and approximate uniformity of synthesized *Albizia Stem Bark Lebbeck* Modified by $Fe_2(MoO_4)_3$ nanocomposite (even in size distribution) can be observed. *Albizia Stem Bark Lebbeck* Modified by

$Fe_2(MoO_4)_3$ nanocomposite after surface modification came to be uneven, bigger and agglomerate**.** It can be seen that the particles are mostly spherical with the various size distribution as they form agglomerates. Based on the particles size distribution, we obtained the average particle size in the range of 40-60 nm very close to those determined by XRD analysis [32,33].

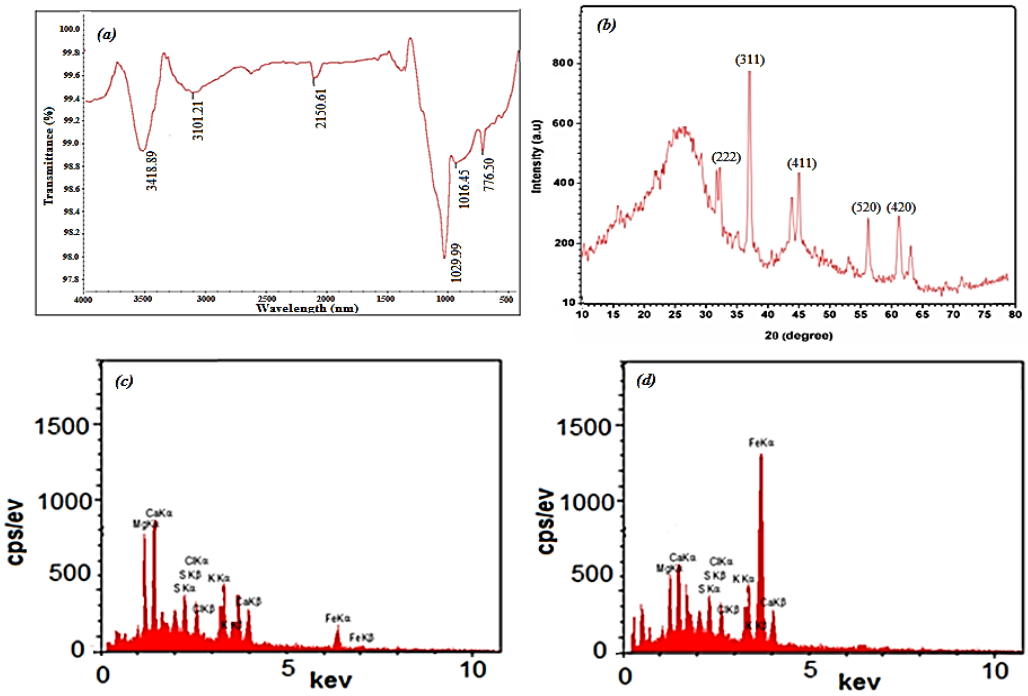

Fig. 4. (a) The IR transmittance spectrum of the prepared *Albizia Stem Bark Lebbeck* Modified by $Fe_2(MoO_4)_3$ nanocomposite (b) XRD of the prepared of *Albizia Stem Bark Lebbeck* Modified by $Fe_2(MoO_4)_3$ nanocomposite (c) EDX spectrum of prepared *Albizia Stem Bark Lebbeck* (d) EDX spectrum of prepared *Albizia Stem Bark Lebbeck* Modified by $Fe_2(MoO_4)_3$ nanocomposite.

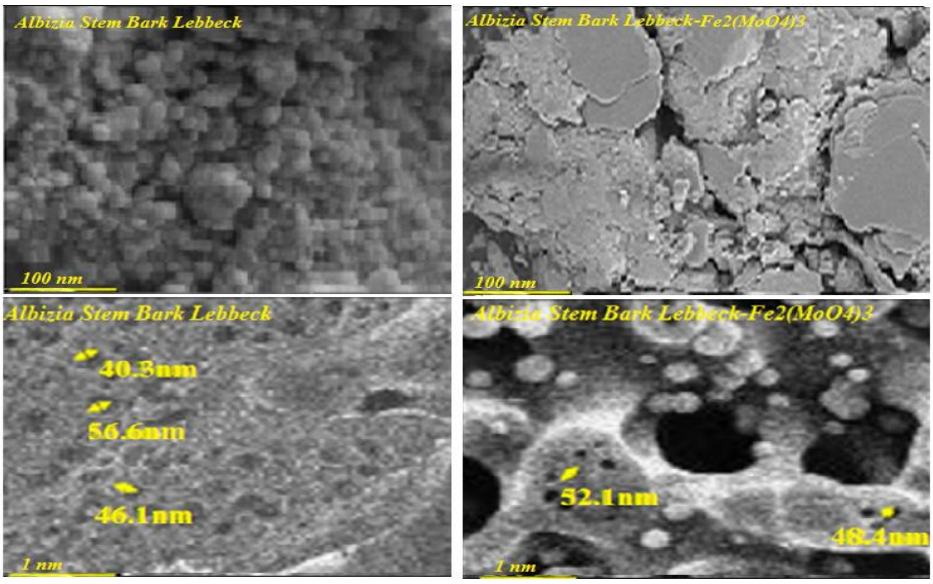

Fig. 5. The SEM image of the prepared *Albizia Stem Bark Lebbeck* Modified by $Fe_2(MoO_4)_3$ nanocomposite in 100 nm and 1nm.

3.2. A comparative study

The adsorption percent of MV dye onto each of $Fe_2(MoO_4)_3$ NPs, *Albizia Stem Bark Lebbeck,* and *Albizia Stem Bark Lebbeck* Modified by $Fe_2(MoO_4)_3$ nanocomposite at the optimum condition, and the obtained results in (Fig. 6) [5,28]. As can see, the trend of the effectiveness of mentioned adsorbents for removing MB from aqueous media is as follows: *Albizia Stem Bark Lebbeck* Modified by $Fe_2(MoO_4)_3$ nanocomposite (99.2%)> *Albizia Stem Bark Lebbeck* (83.7.0%)> $Fe_2(MoO_4)_3$ NPs (71.4%).

3.3. Modeling process

Analyzing accurate data from the RSM is another practical application of Design-Expert STATISTICA 10.0 software. RSM is a statistical method used to perform experiment analysis, modeling, and process optimization. In an RSM model, the response variable (Y) is affected by several independent variables (X_1, X_2, X_3, and X_n). RSM, the most complex model is the second order or quadratic model, which includes the relationship between response and independent variables (contains components such as first power, interactive impacts, polynomial function, and intercept point). The quadratic model by (equation. 3) [34,35].

$$R\%\ (MV)\ dye = 95.709 - 2.1767X_1 - 1.0258X_2 + 0.94833X_3 + 6.3233X_4 + 2.0955X_5 - 1.4350X_1X_2 + 1.3388X_1X_3 + 2.9638X_1X_4 - 1.1638X_1X_5 + 0.69000X_2X_3 + 1.0650X_2X_4 - 1.3900X_2X_5 - 1.6612X_3X_4 + 1.4612X_3X_5 - 1.9138X_4X_5 + 0.66726X_1^2 + 0.91726X_2^2 - 0.020244X_3^2 - 2.8327X_4^2 - 0.41595X_5^2 \quad (3)$$

The value of the determination coefficient for deleting (MV) dye in (Table. 4), it has been noticed that the response surface quadratic model was a befitting model for predicting the function of (MV) dye adsorption on *Albizia Stem Bark Lebbeck* Modified by $Fe_2(MoO_4)_3$ nanocomposite.

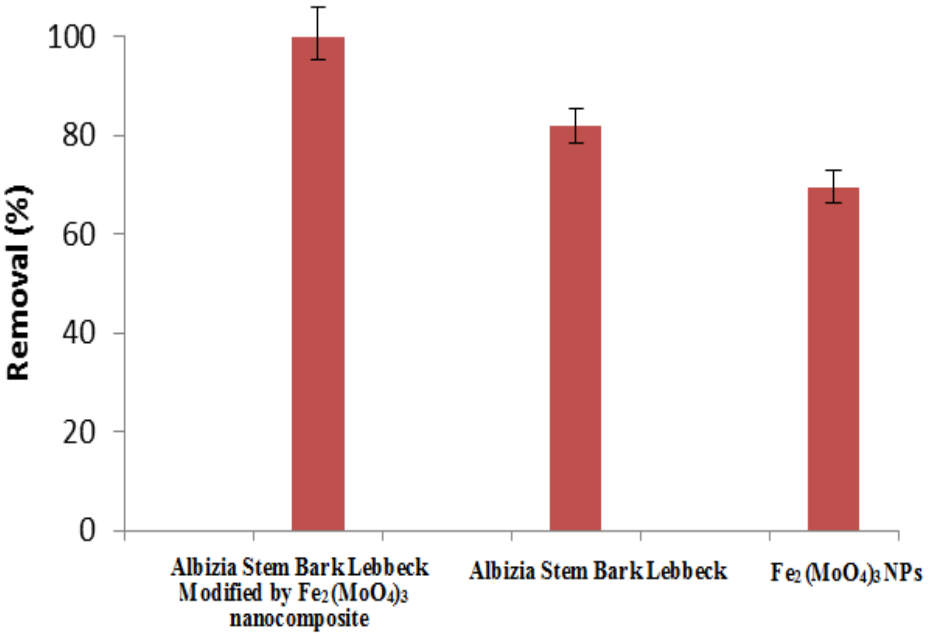

Fig. 6. Comparison of the effectively of $Fe_2(MoO_4)_3$ NPs, *Albizia Stem Bark Lebbeck* and *Albizia Stem Bark Lebbeck* Modified by $Fe_2(MoO_4)_3$ nanocomposite [C_0= 20.0 mgL^{-1}, pH = 5.0, dosage sorbent = 0.03 g, time = 3.0 min].

Table 4. Analysis of Variance for the full quadratic model

Source of variation	DF	(MV) dye			
		Sum square	Mean square	F-value	P-value
Model	14	3105	157.8	22.89	< 0.0001
X_1	1	151.68	151.68	23.64	0.00054
X_2	1	793.2	793.2	112.3	< 0.0001
X_3	1	13.87	13.87	2.2	< 0.0001
X_4	1	31.98	31.98	4.638	0.1705
X_1X_2	1	74.512	74.512	8.78	0.051
X_1X_3	1	33.015	33.015	3.88	0.0476
X_1X_4	1	202.18	202.18	486.87	0.0002
X_2X_3	1	12.78	12.78	31.044	< 0.0001
X_2X_4	1	0.486	0.486	1.1849	0.0105
X_3X_4	1	3.102	3.102	7.521	0.015031
X_3X_5	1	225.63	225.63	545.16	< 0.0001
X_1^2	1	24.53	24.53	2.85	0.11233
X_2^2	1	0.012118	0.012118	0.001389	0.0105
X_3^2	1	234.02	234.02	27.196	0.0178
X_4^2	11	8.330	8.330	1.259	0.2849
Residual	5	72.78	6.611		
Lack of Fit	6	44.05	7.433	1.278	0.3982
Pure Error	31	28.86	5.737		
Cor Total		3082			

3.4. Response surface methodology (RSM) analysis

Response surface methodology (RSM) was utilized to ameliorate the optimization and estimation of all significance interaction of variables and the relative significance of adsorption processes. Fig. 7, exhibits the three-dimensional surface response plots of this interaction. The plots were prepared for a specified pair of factual factors at optimal and fixed values of other variables [35,36]. A positive increase in the (MV) dye removal percentage with the increase in adsorbent mass. Significant diminish in removal percentage of the lower amount of *Albizia Stem Bark Lebbeck* Modified by $Fe_2(MoO_4)_3$ nanocomposite is attributed to the higher ratio of (MV) dye molecules to the vacant sites of the adsorbent. Maximum (MV) dye deletion of 100%, the optimum conditions were as follows: pH of 5.0, ultrasound time of 3.0 min, the adsorbent mass of (0.03 g), and initial (MV) dye equal to 20.0 mgL^{-1}, for (MV) dye. Based on the excellent conformity between the experimental and prediction data, successfully for the evaluation and optimization of the influences of the adsorption independent variables on the removal efficiency of (MV) dye from aqueous media with the help of *Albizia Stem Bark Lebbeck* Modified by $Fe_2(MoO_4)_3$ nanocomposite [37,38].

3.5. Optimization of CCD

The profile for desirable option with the predicted values in the STATISTICA 10.0 software was used for the optimization of the process shown in (Fig. 8). Based on the excellent conformity between the experimental and prediction data, successfully for the evaluation and optimization of the influences of the adsorption independent variables on the removal efficiency of (MV) dye from aqueous media with the help of *Albizia Stem Bark Lebbeck* Modified by $Fe_2(MoO_4)_3$ nanocomposite [37,38].

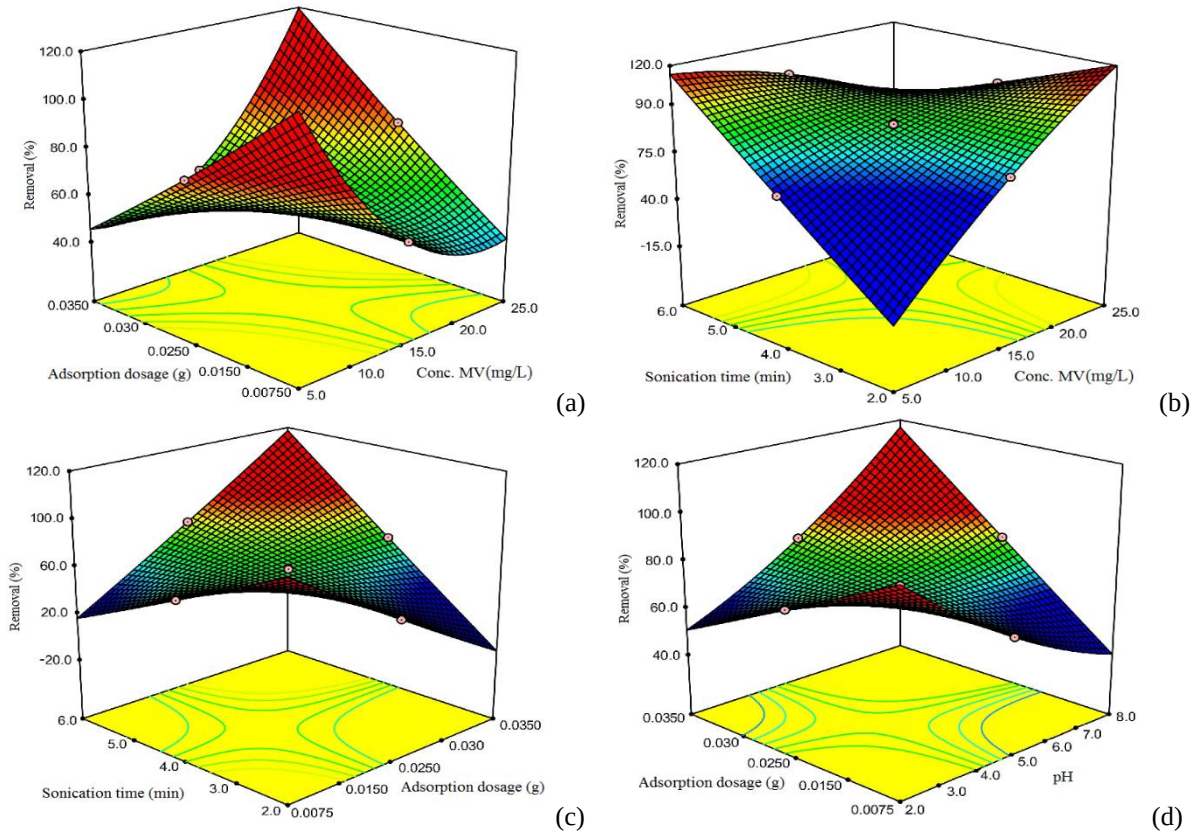

Fig. 7. Response surfaces for the dye removal: (a) adsorbent dosage - initial (MV) dye concentration (b) contact time, initial (MV) dye concentration (c) contact time - adsorbent dosage (d) (MV) dye adsorbent dosage (MV) dye – pH.

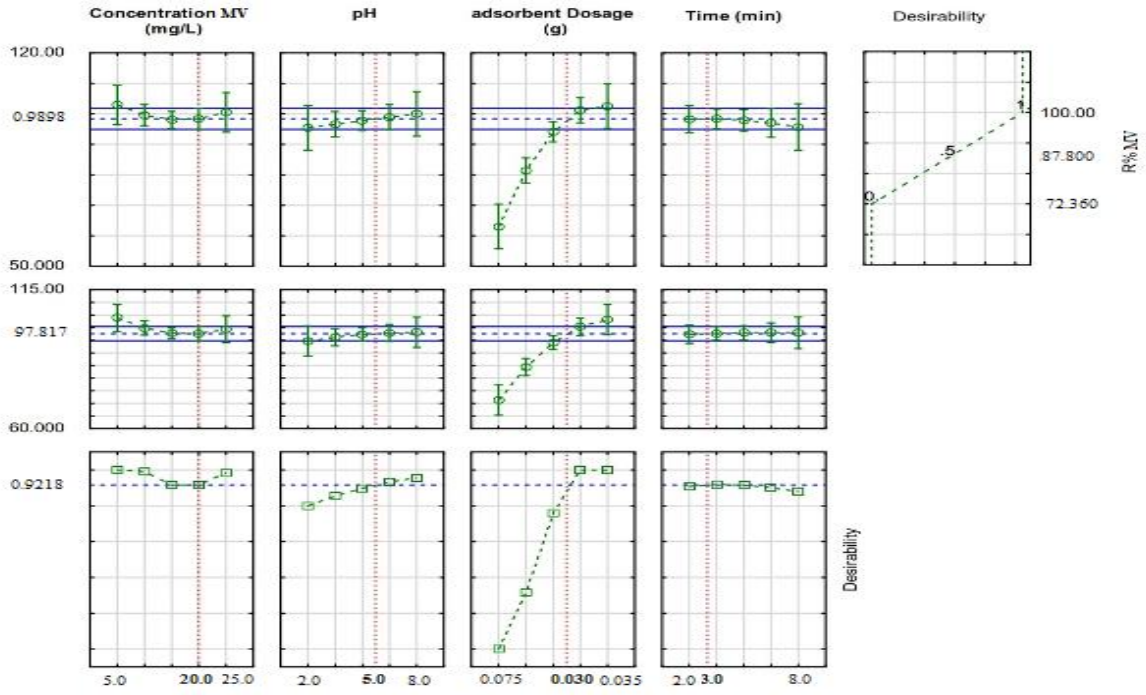

Fig. 8. Profiles values for removal of (MV) dye after optimization.

3.6. Adsorption isotherms

Considering the variation of equilibrium adsorption capacities in terms of the equilibrium concentration (C_e) of the adsorbate, under the optimum values of other parameters, we can examine some suitable isotherms for representing the respect experimental data [39-41]. Fulfill this goal, we compared the experimental results with the three most common isotherm models, including Langmuir, Freundlich, and Temkin isotherms. The nonlinear form of the model was used for fitting the experimental data Table. 5. The respect equations for these models are as follow:

$$q_e = \frac{q_m K_L C_e}{1 + K_L C_e} \quad \text{Langmuir model} \quad (4)$$

$$q_e = q_m K_F^{'} + C_e^{1/n} \quad \text{Freundlich model} \quad (5)$$

$$q_e = q_m (B_T^{'} \ln A_T C_e) \quad \text{Temkin model} \quad (6)$$

q_m represents the maximum value of q_e, which is necessary for the monolayer covering of the whole surface of the used adsorbent. Choose $q_m K_F^{'} = K_F$, the Freundlich model, and $q_m B_T^{'} = B_T$ the Temkin model. The linear equation of the models mentioned above, respectively follows:

$$\frac{1}{q_e} = \frac{1}{q_m K_L C_e} + \frac{1}{q_m} \quad (7)$$

$$\ln q_e = \frac{1}{n} \ln C_e + \ln K_F \quad (8)$$

$$q_e = B_T \ln C_e + B_T \ln A_T \quad (9)$$

3.7. The adsorption kinetics survey

Kinetic models help the evaluate performance of various adsorbents for the removal of dyes. The many kinetic models developed chiefly used are Lagargren's *pseudo*-first-order kinetics and *pseudo*-second-order model [42,43].

The quasi-first-order kinetic model formula is:

$$\ln(q_e - q_t) = \ln q_e - \frac{k_1}{2.303} t \quad (10)$$

The quasi-second-order dynamic model formula is:

$$\frac{t}{q_t} = \frac{1}{k_2 q_e^2} + \frac{t}{q_e} \quad (11)$$

qt and qe are the sorption quantity at time t and equilibrium, respectively, and k is the rate consistent, a plot of t/ q via t gives the *pseudo*-second-order adsorption. *Pseudo*-second-order rate is constant from the respective fields. From the experimental results, the removal of (MV) dye follows the *pseudo*-second-order rate shown in (Table. 6) [45].

Table 5. The adsorption isotherm models of (MV) dye onto *Albizia Stem Bark Lebbeck* Modified by $Fe_2(MoO_4)_3$ nanocomposite. [C_0= 20.0 mgL^{-1}, pH = 5.0, dosage sorbent = 0.03 g, time = 3.0 min, T=25^{0}C].

Isotherm	Parameters	R% (MV) dye
Langmuir	q_m (mgg^{-1})	120.4
	K_L ($L\ mg^{-1}$)	0.489
	R^2	0.9899
Freundlich	1/n	0.54
	K_F $(mg)^{1-n} L^n g^{-1}$	4.06
	R^2	0.9805
Temkin	B_T ($J\ mol^{-1}$)	15.16
	K_T ($L\ mg^{-1}$)	6.875
	R^2	0.9722

Table 6. Various Kinetic constants and their correlation coefficients calculated for the adsorption of (MV) dye onto *Albizia Stem Bark Lebbeck* Modified by $Fe_2(MoO_4)_3$ nanocomposite. [C_0= 20.0 mgL^{-1}, pH = 5.0, dosage sorbent = 0.03 g, time = 3.0 min, T=25^{0}C]

Models	Parameters	R% (MV) dye
Pseudo-first-order kinetic	$k_1(min^{-1})$	1.54
	q_e (mgg^{-1})	98.12
	R^2	0.96.08
Pseudo-second-order kinetic	k_2 (min^{-1})	0.507
	q_e (mgg^{-1})	106.6
	R^2	0.9998
q (exp) (mg g^{-1})		51.45

3.8. Adsorption thermodynamics

Temperature is one of the most important factors in dye removal efficiency by focusing on changes in the nature of the reactions (exothermic or endothermic) to reveal spontaneous and non-spontaneous reactions, parameters can be used in Eqs. (12) and (13) [43,44].

$$\Delta G^{\circ}_{ad} = -RT\ln K_C \quad (12)$$

$$\ln K_C = \frac{\Delta S^{\circ}_{ad}}{R} - \frac{\Delta H^{\circ}_{ad}}{RT} \quad (13)$$

T is temperature in Kelvin. Values of the K_c were calculated at 288.0 at 338.0 K temperatures. ΔG^0 upon be negative indicating that the studied adsorption process is spontaneous in the range of used temperature, $\Delta H^0<0$, indicates that the studies adsorption is exothermic. Based on the magnitude of ΔH^0, we can say that the mentioned adsorption should be physic sorption one, and van der walls interactions are responsible for adsorption taking place. $\Delta S^0<0$, indicates a decrease in randomness that occurs during (MV) dye adsorption onto *Albizia Stem Bark Lebbeck* Modified by $Fe_2(MoO_4)_3$ nanocomposite, which may come from the (MV) dye aggregation on the *Albizia Stem Bark Lebbeck* Modified by $Fe_2(MoO_4)_3$ nanocomposite surfaces. The results seen in (Table. 7) [44,45].

3.9. Adsorption mechanism of (MV) dye into Albizia Stem Bark Lebbeck Modified by $Fe_2(MoO_4)_3$ nanocomposite

The adsorption mechanism of the (MV) dye onto the surface of the *Albizia Stem Bark Lebbeck* Modified by $Fe_2(MoO_4)_3$ nanocomposite can be inferred from the analysis of the FTIR results, in which the presence of functional groups (-O, MoO_4-, and Fe-O) on the surface was confirmed (Fig. 9), shows the various potential interactions that may occur between the (MV) dye and the *Albizia Stem Bark Lebbeck* Modified by $Fe_2(MoO_4)_3$ nanocomposite surface. Interactions are favored owing to the cationic nature of the dye with the negative surface charges of the *Albizia Stem Bark Lebbeck* Modified by $Fe_2(MoO_4)_3$ nanocomposite. Interactions likely involve hydrogen bonding between the acceptor and the donor groups of the *Albizia Stem Bark Lebbeck* Modified by $Fe_2(MoO_4)_3$ nanocomposite –MV dye [12,34]. With π-π interactions between the p–electron system of the *Albizia Stem Bark Lebbeck* Modified by $Fe_2(MoO_4)_3$ nanocomposite structure and the aromatic rings of the (MV) dye molecules. In neutral and weak alkaline conditions, (MV) dye exhibits substantial proton loss and exists as free ions in the solution, thus inhibiting the chemical adsorption to some extent. The structure of *Albizia Stem Bark Lebbeck* Modified by $Fe_2(MoO_4)_3$ nanocomposite, especially

after modification, tempers the negative effect *via* physical adsorption [46].

3.10. Recycling of the adsorbent

The ability to recover, and reusing of the adsorbent was tested in several steps of adsorption, and desorption. The result is shown in (Fig. 10). As shown in Figure, 98% of (MV) dye was desorbed from the adsorbent after the first cycle, and after 6 cycles, there were slight changes in (MV) dye desorption. So, it was concluded that the desired removal of 98% could be achieved after 6 cycles [29,47].

Table 7. The thermodynamic parameters for the adsorption of (MV) dye onto *Albizia Stem Bark Lebbeck* Modified by $Fe_2(MoO_4)_3$ nanocomposite. [C_0= 20.0 mgL^{-1}, pH = 5.0, dosage sorbent = 0.03 g, time = 3.0 min]

Dye	T (^{O}K)	Kc	ΔG^{o}(kJ/mol)	ΔH^{o}(kJ/mol)	ΔS^{o} (kJ/mol K)
(MV) dye (20 mgL^{-1})	288	47.5	-9.26	-29.24	-131.49
	308	57.2	-10.36		
	318	96.3	-12.08		
	328	145	-13.57		
	338	291	-15.94		

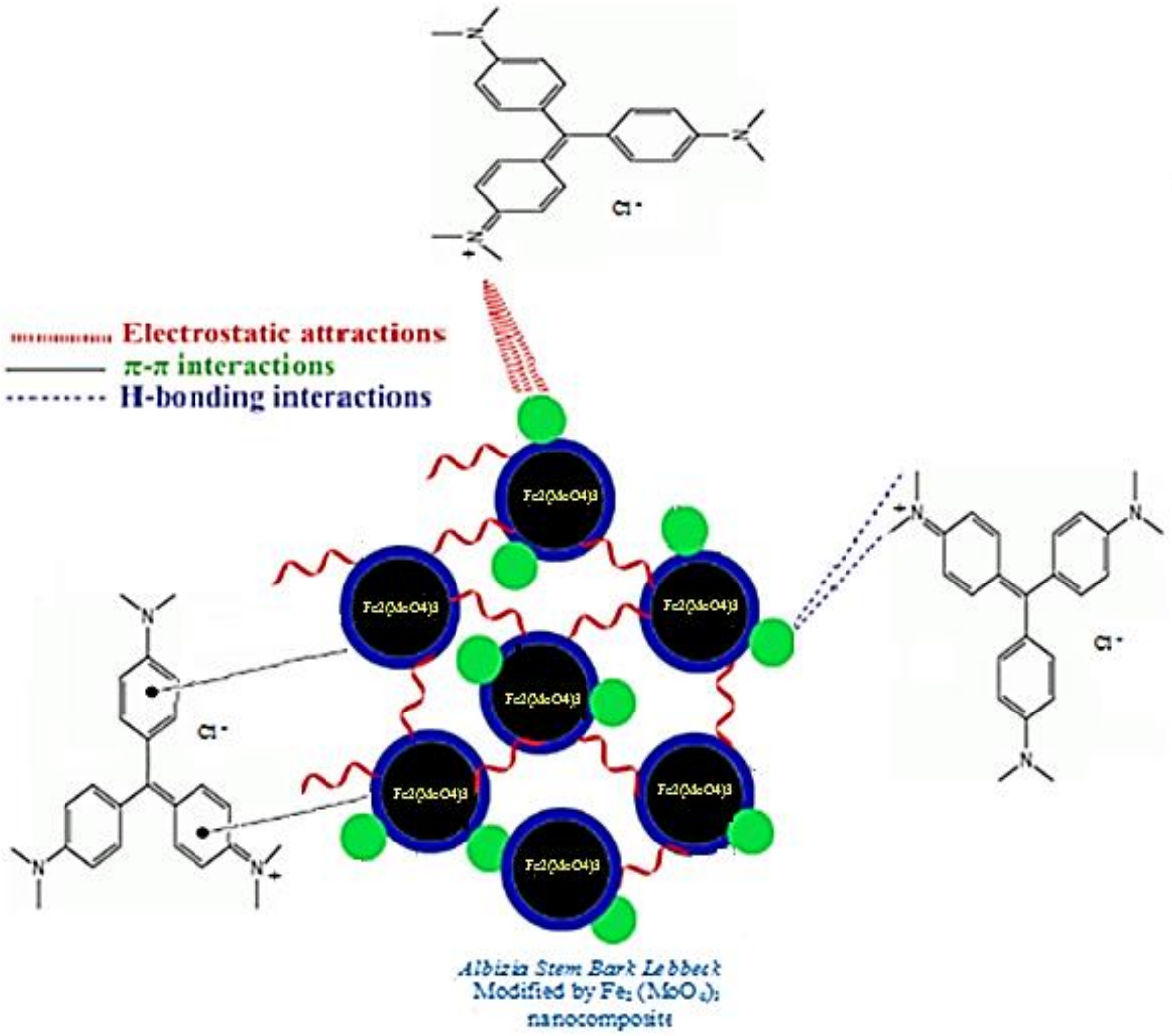

Fig. 9. Illustration of the possible interaction between (MV) dye and surface *Albizia Stem Bark Lebbeck* Modified by $Fe_2(MoO_4)_3$ nanocomposite.

3.11. Comparison of various adsorbent

A comparison of the maximum adsorption capacities of different adsorbents for the removal of (MV) dye was also reported in (Table. 8). The outcomes of the table clearly show that the sorption capacity of utilized sorbent in the current study is significantly high, and adsorption capacity, and contact time in this article is superior to other adsorbents to remove (MV) dye. In general, morphology, particle size and distribution and surface structure of this sorbent were effective in its successful outcomes.

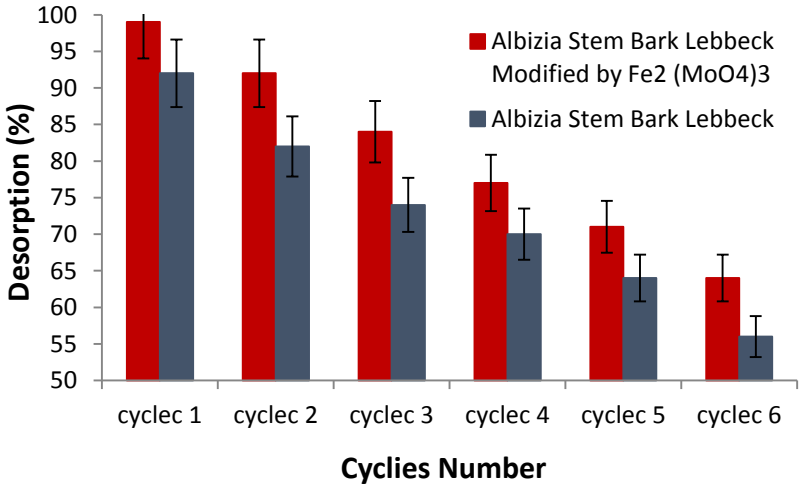

Fig. 10. Desorption of (MV) dye from *Albizia Stem Bark Lebbeck* Modified by $Fe_2(MoO_4)_3$ nanocomposite. [C_0= 20.0 mgL^{-1}, pH = 5.0, dosage sorbent = 0.03 g, time = 3.0 min, T=25^{0}C].

Table 8. Comparison of results for this work with other reported.

Dye	Adsorbent	Dosage sorbent	pH	Time	Adsorption capacity	References
Methyl Violet (MV)	sawdust/Fe_3O_4 composite	0.28 g	9.0	50 min	46.8 mgg^{-1}	[1]
Methyl Violet (MV)	HNT-Fe_3O_4 composite	0.15 g	5.0	10 min	20.04 mgg^{-1}	[6]
Methyl Violet (MV)	β-cyclodextrin onto mesoporous silica	0.05 g	6.0	5 min	34.5 mgg^{-1}	[7]
Methyl Violet (MV)	Peanut straw charRice	0.5 g	5.0	30 min	101.01, 48.64 and 70.36 mgg^{-1}	[8]
Methyl Violet (MV)	Sanctae-Crucis	2.0 g	8.0	80 min	10.2 mgg^{-1}	[9]
Methyl Violet (MV)	Acid modified activated carbon	0.1 g	7.0	25 min	83.3 mg g^{-1}	[45]
Methyl Violet (MV)	*Albizia Stem Bark Lebbeck* Modified by $Fe_2(MoO_4)_3$ nanocomposite	0.03 g	5.0	3 min	120.4 mgg^{-1}	This work

4. CONCLUSION

In this study, a thorough investigation was performed on the effectiveness of synthesized *Albizia Stem Bark Lebbeck* Modified by $Fe_2(MoO_4)_3$ nanocomposite as an adsorbent for the deletion of (MV) dye from industrial wastewater. In this research, the values of 20 $mg.L^{-1}$, 0.03 g, 5.0, and 3.0 min, the ideal values for (MV) dye concentration, adsorbent mass, pH, and contact time, respectively. Adsorption equilibrium and kinetic data were fitted with the Langmuir monolayer isotherm model (q: 0.9899) and *pseudo*-second-order kinetics (R^2: 0.999). Thermodynamic parameters (ΔG°: -9.26 kJ mol^{-1}, ΔH°: -29.24 kJ mol^{-1}, ΔS°: -131.49 kJ $mol^{-1}K^{-1}$) also indicated Methyl Violet dye adsorption is feasible, spontaneous, and exothermic. The adsorbent was recyclable more than once and obtained an ideal adsorption capacity (120.4 mgg^{-1}), for Methyl Violet dye. According to the results, *Albizia Stem Bark Lebbeck* Modified by $Fe_2(MoO_4)_3$ nanocomposite could as a reusable adsorbent, it would be an economically viable option that can lead to industrial wastewater advancement and high-quality treated effluent.

ACKNOWLEDGEMENT

The authors gratefully acknowledge support of this work by the Islamic Azad University, Branch of Kermanshah, Iran.

DISCLOSURE STATEMENT

No potential conflict of interest was reported by the author(s).

REFERENCES

[1] H. Pooladi, R. Foroutan, H. Esmaeili, Synthesis of wheat bran sawdust/Fe_3O_4 composite for the removal of methylene blue and methyl violet, Environ. Monitor. Assessment. 193(5) (2021) 1-19.

[2] L .P. Lingamdinne, H. R. Koduru, R. R. Karri, A comprehensive review of applications of magnetic graphene oxide based nanocomposites for sustainable water purification, J. Environ. Manage. 231 (2019) 622-634.

[3] M. Pirsaheb, M. Moradi, H. R. Ghaffari, K. Sharafi, Application of response surface methodology for efficiency analysis of strong non-selective ion exchange resin column (A 400 e) in nitrate removal from groundwater, Int. J. Pharma. Technol. 8(1) (2016) 11023-11034.

[4] T. Tatarchuk, N. Paliychuk, R. Babu Bitra, A. Shyichuk, Mu. Naushad, I. Mironyuk, D. Ziolkovska, Adsorptive removal of toxic Methylene Blue and Acid Orange 7 dyes from aqueous medium using cobalt-zinc ferrite nanoadsorbents, Desal. Water Treat. 150 (2019) 374-385.

[5] Sh. Ghanavati Nasab, A. Semnani, A. Teimouri, H. Kahkesh, T. Momeni Isfahani S. Habibollahi, Removal of Congo Red from Aqueous Solution by Hydroxyapatite Nanoparticles Loaded on Zein as an Efficient and Green Adsorbent: Response Surface Methodology and Artificial Neural Network-Genetic Algorithm, J. Polymers Environ. 26(9) (2018) 3677. https://doi.org/10.1007/s10924-018-1246-z.

[6] M. R. R. Kooh, M.K. Dahri, L. B. L. Lim, Removal of the methyl violet 2B dye from aqueous solution using sustainable adsorbent Artocarpus odoratissimus stem axis, J. Appl. Water Sci. 7 (2017) 3573-3581.

[7] K. Liu, H. Liu, L. Li, W. Li, J. Liu, T. Tang, Adsorption of methyl violet from aqueous solution using β-cyclodixtrin immobilized onto mesoprous silica, Supramol. Chem. 33(4), (2021) 1-19.

http://doi.org.1080/10610278.2021.1917574.

[8] R. K. Xu, S. C. Xiao, J. H. Yuan, A. Z. Zhao, Adsorption of methyl violet from aqueous solutions by the biochars derived from crop residues, Bioresource Technol. 102(22) (2011) 10293-10298.

[9] R. Mahini, H. Esmaeili, H. Foroutan, Adsorption of methyl violet from aqueous solution using brown algae Padina sanctae-crucis, Turk. J. Biochem. 24 (2018) 1-12.

[10] A. H. Jawad, N. N. M. Firdaus Hum, A.S. Abdulhameed, M.Z. Mohd Ishak, Mesoporous activated carbon from grass waste via H_3PO_4-activation for methylene blue dye removal: modelling, optimisation, and mechanism study, Int. J. Environ. Anal. Chem. 100 (2020) 1-18. https://doi.org/10.1080/03067319.2020.1807529.

[11] N. N. Abd Malek, A. H. Jawad, A. S. Abdulhameed, K. Ismail, B. H. Hameed, New magnetic Schiff's base-chitosan-glyoxal/fly ash/Fe_3O_4 biocomposite for the removal of anionic azo dye: An optimized process, Int. J. Biolog. Macromolecules. 146 (2020) 530–539.

[12] A. H. Jawad, A. S. Abdulhameed, S. V. Surip, S. Sabar, Adsorptive performance of carbon modified chitosan biopolymer for cationic dye removal: kinetic, isotherm, thermodynamic, and mechanism study, Int. J. Environ. Anal. Chem. 100 (2020) 1-20. DOI: 10.1080/03067319.2020.1807966.

[13] S. H. Ahmadi, P. Davar, A. Manbohi, Adsorptive Removal of Reactive Orange 122 from Aqueous Solutions by Ionic Liquid Coated Fe_3O_4 Magnetic Nanoparticles as an Efficient Adsorbent, Iran. J. Chem. Chem. Eng. 35 (2016) 63-73.

[14] A. Dalvand, N. Golchinpoor, S. S. Hosseini, E. Gholibegloo, M.R. Ganjali, M. Khazaei, A.H. Mahvi, H. Kamani, Comparison of Moringa stenopetala seed extract as a clean coagulant with Alum and Moringa stenopetala-Alum hybrid coagulant to remove direct dye from Textile Wastewater, Environ. Sci. Pollut. Res. 23 (2016) 16396-16405. DOI 10.1007/s11356-016-6708-z.

[15] Sh. Ghanavati Nasab, A. Semnani, A. Teimouri, M. Javaheran Yazd, T. Momeni Isfahani, S. Habibollahi, Decolorization of crystal violet from aqueous solutions by a novel adsorbent Chitosan/nanodiopside using response surface methodology and artificial neural network-genetic algorithm, Int. J. Biology. Macromolecules. 124 (2019) 429-456. https://doi.org/10.1016/j.ijbiomac.2018.11.148.

[16] Z. Jafari Harandi, Sh. Ghanavati Nasab, A. Teimouri, Synthesis and characterisation of magnetic activated carbon/diopside nanocomposite for removal of reactive dyes from aqueous solutions: experimental design and optimization, Int. J. Environ. Anal. Chem. 99(6) (2019) 568-584. https://doi.org/10.1080/03067319.2019.1597867.

[17] C. Li, S. Farrokhpay, K. Runge, F. Shi, Effect of flotation froth properties on froth rheology, Powder Technol. 287 (2016) 216-255.

[18] M. Abniki, A. Moghimi, Synthesis of chitosan functionalized magnetic carbon nanotubes for dispersive solid-phase extraction of bromocresol green, Micro Nano Lett. 16 (2021) 455-462.

https://www.researchgate.net/publication/353273049.

[19] A. Karami, K. Sharafie, K. Karimyan, Sh. Rahimi, R. Davoodi, T. Khosravi, M. Karimaei, M. Miri, H. Sharafi, A. Azari, Application of response surface methodology for statistical analysis, modeling, and optimization of malachite green removal from aqueous solutions by manganese-modified pumice adsorbent, Desal. Water. Treat. 89 (2017) 150-161.

[20] A. Reghioua, D. Barkat, A. H. Jawad, A. S. Abdulhameed, M. R. Khan, Synthesis of Schiff's base magnetic crosslinked chitosan-glyoxal / ZnO/Fe_3O_4 nanoparticles for enhanced adsorption of organic dye: Modeling and mechanism study, Sustaina. Chem. Pharma. 20 (2021) 100379.

[21] A. Reghioua, D. Barkat, A. H. Jawad, A. S. Abdulhameed, A. A. Al-Kahtani, Z. A. ALOthman, Parametric optimization by Box–Behnken design for synthesis of magnetic chitosan-benzil/ZnO/Fe_3O_4 nanocomposite and textile dye removal, J. Environ. Chem. Eng. 9 (2021) 105166.

[22] H. Esmaeilli, R. Foroutan, D. Jafari, Effect of interfering ions on phosphate removal from aqueous media using magnesium oxide@ferric molybdate nanocomposite, Korean. J. Chem. Eng. 37(5) (2020) 804-816. .

[23] R. Foroutan, S.J. Peighambardoust, S. Hemmati, Preparation of clinoptilolite /starch/$CoFe_2O_4$ magnetic nanocomposite powder and its elimination properties for cationic dyes from water and wastewater, Int. J. Biolog. Macromolecules. 189 (2021) 432-445.

[24] F. Marahel, B. Mombeni Goodajdar, N. Basri, L. Niknam, A. Ghazali, Applying Neural Network Model for Adsorption Methyl Paraben (MP) dye Using Ricinus Communis-capeed Fe_3O_4NPs Synthesized from Aqueous Solution, Iran. J. Chem. Chem. Eng. 41 (2022) 1-18. doi: 10.30492/IJCCE.2021.527025.4636.

[25] K. Sharafi, M. Pirsaheb, V. K. Gupta, Sh. Agarwal, M. Moradi, Y. Vasseghian, E.N. Dragoi, Phenol adsorption on scoria stone as adsorbent-Application of response surface method and artificial neural networks, J. Mol. Liq. 274(15) (2019) 699-714.

[26] M. Rahmani Piani, M. Abrishamkar, B. Mombeni Goodajdar, M. Hossieni, Trihalomethanes (THMs) removal from aqueous solutions using environmental friendly and effective adsorbent onto Mespilus germanica modified by $Fe_2(MoO_4)_3$ nanocomposite on equilibrium, thermodynamic, and kinetics, Desal. Water Treat. 223 (2021) 288- 302.

[27] M. Ullah, R. Nazir, M. Khan, W. Khan, M. Shah, S.G. Afridi, The effective removal of heavy metals from water by activated carbon adsorbents of Albizia lebbeck and Melia azedarach seed shells, J. Soil and Water Res. 15 (2020) 30-37. https://doi.org/10.17221/212/2018-SWR.

[28] A. Rafiee, Sh. Ghanavati Nasab, A. Teimouri, Synthesis and characterization of pistachio shell/ nanodiopside nanocomposite and its application for removal of Crystal Violet dye from aqueous solutions using central composite design, Int. J. Environ. Anal. Chem. 99 (2019) 1-26. https://doi.org/10.1080/03067319.2019.1655556.

[29] L. Dos Reis Darcie, B. V. Jacon, G. S. Silva Andrade, A. M. Siqueira Oliveira, M. S. Lopes, T. R. Giraldi, Eucalyptus sawdust as an alternative adsorbent for rhodamine B dye

removal, Desal. Water Treat. 229 (2021) 430-440.

[30] F. Marahel, B. Mombeni Goodajdar, L. Niknam, M. Faridnia, E. Pournamdari, S. Mohammad Doost, Ultrasonic Assisted Adsorption of Methylene Blue Dye and Neural Network Model for Adsorption of Methylene Blue Dye by Synthesized Mn-doped PbS nanoparticles, Int. J. Environ. Anal. Chem. 101 (2021) 1-22. https://doi.org/10.1080/03067319.2021.1901895.

[31] H. S. Ghazi Mokri, N. Modirshahla, M. A. Behnajady, B. Vahid, Adsorption of C.I. Acid Red 97 dye from aqueous solution onto walnut shell: kinetics, thermodynamics parameters, isotherms, Int. J. Environ. Sci. Technol. 12 (2015) 1401-1408.

[32] S. Mahdi Hadi, M. K. H. Al – Mashhadani, M. Y. Eisa, Optimization of dye adsorption process for Albizia lebbeck pods as a biomass using central composite rotatable design model, Chem. Ind. Chem. Eng. Q. 25 (2019) 39-46.

[33] G. K. Sharma, N. Dubey, Review of Shirish (Albizia lebbeck) therapeutic properties, Int. J. Ayur. Herbal Med. 5 (2015) 1683-1688.

[34] A. H. Jawad, A. S. Abdulhameed, L. D. Wilson, S.S.A. Syed-Hassan, Z. A. ALOthman, M. Rizwan Khan, High surface area and mesoporous activated carbon from KOH-activated dragon fruit peels for methylene blue dye adsorption: Optimization and mechanism study, Chinese J. Chem. Eng. 32 (2021) 281-290. https://doi.org/10.1016/j.cjche.2020.09.070.

[35] F. Mohammadi, A. Esrafili, H. R. Sobhi, M. Behbahani, M. Kermani, E. Asgari, Z. Rostami Fasih, Evaluation of adsorption and removal of methylparaben from aqueous solutions using amino-functionalized magnetic nanoparticles as an efficient adsorbent: Optimization and modeling by response surface methodology (RSM), Desal. Water Treat. 103 (2018) 248-260.

[36] M. Pargari, F. Marahel, B. Mombini Godajdar, Ultrasonic Assisted Adsorption of Propyl Paraben on Uultrasonically Synthesized TiO_2 nanoparticles loaded on activated carbon: Optimization, kinetic and equilibrium studies, Desal. Water Treat. 212 (2021) 164-172.

[37] M. Kiani, S. Bagheri, A. Khalaji, N. Karachi, Ultrasonic supported deletion of Rhodamine B on ultrasonically synthesized zinc hydroxide nanoparticles on activated carbon concocted from wood of cherry tree: experimental design methodology and artificial neural network, Desal. Water Treat. 226 (2021) 147-156.

[38] S. Hajati, M. Ghaedi, B. Barazesh, F. Karimi, R. Sahraei, A. Daneshfar, A. Asghari, Application of high order derivative spectrophotometry to resolve the spectra overlap between BG and MB for the simultaneous determination of them: ruthenium nanoparticle loaded activated carbon as adsorbent, J. Ind. Eng. Chem. 20 (2014) 2421–2427.

[39] L. Daneshvar, A. Nezamzadeh-Ejhieh, Photocatalytic activity of ZnO nanoparticles towards tinidazole degradation: Experimental design by response surface methodology (RSM), Desal. Water Treat. 141 (2019) 364-376.

[40] Y. Yang, Y. Xie, L. Pang, M. Li, X. Song, J. Wen, H. Zhao, Preparation of reduced graphene oxide/poly (acrylamide) nanocomposite and its adsorption of Pb^{2+} and methylene

blue, Langmuir. 29 (2013) 10727-10736.
[41] M. Kiani, S. Bagheri, N. Karachi, E. Alipanahpour Dil, Adsorption of purpurin dye from industrial wastewater using Mn-doped Fe_2O_4 nanoparticles loaded on activated carbon, Desal. Water. Treat. 152 (2019) 366-373.
[42] M. Hubbe, S. Azizian, S. Douven, Implications of Apparent Pseudo-Secound-Order Adsorption Kinetics onto Cellulosic Materials: A Review, Bio Resources. 14(3) (2019) 7582-7626.
[43] A. Asfaram, M. Ghaedi, S. Hajati, A. Goudarzi, Synthesis of magnetic γ-Fe_2O_3-based nanomaterial for ultrasonic assisted dyes adsorption: Modeling and optimization, Ultrason - Sonochem. 32 (2016) 418-431.
[44] F. Marahel, Adsorption of Hazardous Methylene Green Dye from Aqueous Solution onto Tin Sulfide Nanoparticles Loaded Activated Carbon: Isotherm and Kinetics Study, Iran. J. Chem. Chem. Eng. 38(5) (2019) 129-142.
[45] A. T. M. Din, B. H. Hameed, Adsorption of methyl violet dye on acid modified activated carbon: isotherms and thermodynamics, J. Appl. Sci. Environ. Sanita. 5(2) (2010) 161-170.
[46] A. S. Abdulhameed, N. N. M. Firdaus Hum, S. Rangabhashiyam, A.H. Jawad, L. D. Z. Wilson, M. Yaseen, A. A. Al-Kahtani, Z. A. ALOthman, Statistical modeling and mechanistic pathway for methylene blue dye removal by high surface area and mesoporous grass-based activated carbon using K_2CO_3 activator, J. Environ. Chem. Eng. 9 (2021) 105530. https://doi.org/10.1016/j.jece.2021.105530.
[47] E. Mousavi, A. Geramizadegan, Adsorption of Benzyl Paraben Dye from Aqueous Solutions Using synthesized Mn-doped PbS (PbS:Mn) nanoparticles, J. Phys. Theore. Chem. 17(3,4), (2020) 123-143.

مجله شیمی فیزیک و شیمی نظری
دانشگاه آزاد اسلامی واحد علوم و تحقیقات
جلد ۱۸، شماره ۴، زمستان ۱۴۰۰
ISSN ۱۷۳۵-۲۱۲۶

روش پاسخ سطح برای حذف رنگ متیل ویولت با استفاده از پوست ساقه درخت گل ابریشم اصلاح شده توسط نانو کامپوزیت مولیبدات آهن از فاظلاب صنعتی

شیوا عین القضاتی[۱]، الهام پورنامداری[۲] *، نسرین چوبکار[۱] و فرزانه مراحل[۳]

[۱] دانشگاه آزاد اسلامی واحد کرمانشاه، گروه مهندسی کشاورزی گرایش محیط زیست، واحد کرمانشاه، ایران
[۲] دانشگاه آزاد اسلامی واحد اسلامشهر، گروه مهندسی شیمی، واحد اسلامشهر، ایران
[۳] دانشگاه آزاد اسلامی واحد امیدیه، گروه مهندسی شیمی، واحد امیدیه، ایران

چکیده

کاربرد **پوست ساقه درخت گل ابریشم اصلاح شده توسط نانو کامپوزیت مولیبدات آهن**، برای حذف رنگ متیل ویولت از پساب صنعتی مورد مطالعه قرار گرفت. تکنیک‌های یکسانی از جمله (IR، XRD و SEM) برای توصیف این ماده جدید استفاده شده‌اند. اثرات متغیرهایی از جمله غلظت اولیه متیل ویولت (X_1)، pH (X_2)، دوز جاذب (X_3)، و زمان فراصوت (X_4) با استفاده از طراحی مرکب مرکزی (CCD) تحت روش سطح پاسخ (RSM) مورد بررسی قرار گرفت. مقادیر ۲۰ میلی گرم در لیتر، ۰/۰۳ گرم، ۵/۰، ۳/۰ دقیقه به ترتیب به عنوان مقادیر ایده آل برای غلظت متیل ویولت، جاذب، pH و زمان تماس در نظر گرفته شد. تعادل جذب و داده های جنبشی به ترتیب با مدل ایزوترم تک لایه لانگمویر و سینتیک شبه مرتبه دوم با حداکثر ظرفیت جذب (۱۲۰/٤ میلی گرم بر گرم) برازش شدند. پارامترهای ترمودینامیکی ($\Delta H°$: 29.24 kJ mol^{-1}، $\Delta G°$: -9.26 kJ mol^{-1}، $\Delta S°$: -131.49 kJ mol^{-1} K^{-1})، همچنین نشان داد که جذب متیل ویولت امکان پذیر، خود به خود و گرمازا است. نتایج کلی تایید کرد که **پوست ساقه درخت گل ابریشم اصلاح شده توسط نانو کامپوزیت مولیبدات آهن** یک جاذب موثر برای حذف رنگ های سمی از فاضلاب است.

کلید واژه‌ها: رنگ متیل ویولت، ظرفیت جذب، طراحی مرکب مرکزی (CCD)، روش پاسخ سطح (RSM)، فاضلاب صنعتی

* مسئول مکاتبات: elhampurnamdari@gmail.com